

The UDel Models - MANET Mobility and Path Loss in an Urban/Suburban Environment

Abstract

It is well known that mobility plays an important role in the performance of MANET protocols. Investigations of the impact of physical layer indicates that the physical layer also plays an important role. This paper presents tools for modeling the environment for MANETs. This environment is defined in terms of buildings, offices, hallways, sidewalks, and roads. Within this environment, the movements of pedestrians, cars, and helicopters/UAVs are modeled. Tightly coupled to the modeled environment is a model of the behavior of links, in particular, the path loss. The mobility is composed of different types of mobility models including graph-based random waypoint and graph-based random walk. The path loss is found with a mixture of beam tracing and an attenuation factor model. The path loss model accounts for reflections from the walls of buildings as well as the penetration into and out of buildings. This paper also includes some illustrative examples of propagation and briefly looks at the impact of these models on the performance of MANET routing protocols. The tool developed is compatible with the QualNet simulator (after a small change) and is available for download.

I. INTRODUCTION

Arguably the two most critical features of MANETs are that the nodes are mobile and the links between nodes are subject to breakage and transmission error. This paper introduces a new simulation tool that focuses on realistic modeling of these two aspects of MANETs. Moreover, this tool allows the environment to be included into MANET simulation. The environment includes urban and suburban features such as buildings, sidewalks, and roads. Within this environment, pedestrian mobile nodes move from office to office through hallways and along sidewalks, while vehicle nodes move along roads and aircraft move anywhere in the three dimensional space above the city. Coupled to this environment model of mobility is a model of radio propagation. As any mobile phone user knows, the propagation of radio signals is complex with "holes" seeming to appear and disappear at random. While it is well appreciated that wireless links are subject to great variations and it is intuitive that the performance of MANETs is greatly dependent on the behavior of the wireless links, it is somewhat surprising that more realistic propagation models are rarely used.

When a radio wave hits an object that is much larger than the wavelength (12.5cm for 2.4GHz), much of the energy of the wave is reflected in a direction that obeys Snell's law. As a result, in an urban or suburban environment, radio waves can make a considerable number of reflections before reaching their destination. In this way, the buildings and other reflective objects in the vicinity of a radio transmission play a critical role. Hence, one cannot discuss a realistic propagation model without considering these reflective objects. As will be discussed in Section III, while the stochastic models typically used in communication theory provide a useful way to compare communication algorithms, they should not be used when trying to evaluate protocols for MANETs. Rather, deterministic models for propagation must be used. Thus, in order to have a realistic model for propagation, one must also model the buildings and other reflective objects.

Along with a propagation model, the UDel models include a new mobility model. The motivation for the new mobility models is that the propagation model requires that objects such as buildings be simulated. Thus, the mobile nodes must navigate around and into buildings. For example, today's mobility models do not specify things such as which floor the node is on. This paper develops a suitable mobility model. However, other models are also possible and will be developed in the future.

In order to gain an understanding of the importance of the models presented, consider Figure 7, which shows the signal strength at different locations. It is apparent that the signal strength can vary in a nonhomogeneous way. For example, in some regions the signal strength varies slowly, whereas in other areas, the signal strength varies drastically over short distances. Another, perhaps less apparent aspect is that this type of propagation will lead to significantly different topologies. For example, nodes encircled by a set of completely connected nodes need not be connected to nodes that encircle them. Considering floors of a building, the propagation models show that in some settings the best connections between floors may be long paths that use outdoor nodes as a relays. Also, standard assumptions about link behavior might not hold in this environment. For example, in [2] it is suggested that node

velocities can be used to predict the residual lifetime of a link. Similarly, in [3], it is suggested that signal strength can be used to predict the residual lifetime of a link, while [4] and [5] assumed that position and connectivity are tightly related. However, considering that a small movement could potentially lead to a large reduction in signal strength and connectivity, these assumptions need to be reassessed.

While the models presented seem realistic, there is a significant drawback to this modeling approach. Specifically, these models can only be scenario specific. That is, the performance depends on the locations of buildings and the mobility model used. It is not clear if this will, in the end, result in a better simulator. Recall that the goal of a MANET simulator is not necessarily to be realistic, but to stress the protocols in such a way that the protocol that performs the best in the simulator will perform the best in reality. Furthermore, the simulator should provide insight into critical aspects of the behavior of MANETs. Exactly which simulation scheme provides the most meaningful stress and insight is a matter of ongoing research. Therefore, the models presented here should not be used instead of the mobility models in current use, but used in conjunction with them.

The rest of the paper proceeds as follows. In the next section a very brief discussion of current mobility models is given. Then, in Section III, a brief overview of propagation models is given. There, special consideration is given to distinctions between the propagation models useful for MANETs and those used in communication theory. In Section V, the main aspects of the UDel mobility model are discussed. Section VI presents the propagation model and its implementation. Section VII contains some illustrative examples of the propagation found by this model. Section VIII provide a brief look at the performance of MANETs under these models. Section IX provides concluding remarks and some discussion of ongoing and future work in this area.

II. MOBILITY MODELS FOR MANETS

Several mobility models have been suggested for MANET simulation. [6] provides a review of some of these models. Perhaps the most widely used mobility model is random waypoint [7]. This model restricts movement of the mobile nodes to a rectangle. Each node picks a destination within the rectangle along with a speed. The node travels to the destination at that speed. Upon reaching the destination, the node selects and waits for a uniformly distributed pause time. After waiting, the node picks another destination and another speed, continuing the process. The parameters of this model are the minimum and maximum speed and the maximum pause time. It is not uncommon that the speeds range from 0 to 20meters/sec.¹.

Besides random waypoint, there are several other models that guide nodes along random paths through a rectangle. These include Random Walk Mobility Model which selects directions and speeds at random [6] and Gauss-Markov Mobility Model [8].

Another class of models are those that restrict nodes to a graph. These can be subdivided into graph-based random walk model and graph-based random waypoint model. In a graph-based random walk model, the nodes move from vertex to vertex, selecting its next destination at random from the neighboring vertices. A graph-based random waypoint model selects a destination at random from all destinations. The node then moves along the graph to the destination vertex. In most cases, the speed of the node is selected at random and the pauses may occur when the destination is reached. The Manhattan mobility model is a graph-based random walk [9] where nodes are restricted to a dimensional lattice. The City Section model is similar to Manhattan, but uses random waypoint and restricts the speed of the nodes to resemble model traffic moving along city streets. Another graph-based random waypoint model is presented in [10]., where the graph was defined by a Voronoi diagram of obstacles. This graph was further extended to include the vertices of the center point of the obstructions and arcs that emanate from the center of the obstruction to the arcs of the Voronoi diagram. In Section V, we present two graph-based mobility models, a random walk and random waypoint.

Other classes of model are group mobility [11] and Scenario based models [12]. Future versions on the UDel models will include such classes of mobility.

The importance of mobility models has been well documented. In [6], it was shown that the performance under a random direction mobility model is vastly different from that under a random waypoint mobility. In [12], a

¹However, in [?] it was shown that in order for the mobility to reach equilibrium, the speed should have a lower bound greater than zero.

dependence on mobility was also demonstrated. For example, it was shown that in some settings, DSDV achieved higher throughput than DSR. Many papers show a variation in the performance as a function of pause time. [9] and [13] study in detail how mobility affects the performance of MANET routing protocols. Furthermore, the mobility models, while simple, may behave unexpectedly. For example, in [14] it was observed that random waypoint tends to concentrate nodes in the center of the region. On the other hand, [15] showed that in slightly different settings, the locations of the nodes are roughly uniformly distributed.

III. REVIEW OF PROPAGATION MODELS

While it is well known that the mobility model utilized effects performance of the protocol there has been little investigation into the effect of the physical layer. One exception is [16] where it was shown that the performance ranking of routing protocols is influenced by the choice of physical layer model. Specifically, DSR was shown to work better when one physical layer was used, while AODV was shown to work better when another model was used. The physical layer utilized in the UDel model is quite different from those used in [16]. Here we discuss these models as well as others found in the communication literature. It will be argued that, while these models may be well suited for narrow band physical layer design and have gain some popularity in MANETs, they are not appropriate. This section only provides a brief discussion of propagation model; see [17] and [18] for details on propagation modeling.

While there has been extensive work on modeling propagation, much of this work has focused on model the physical layer used in mobile phones. There are significant differences between the communication techniques used in mobile phones and those used in MANETs, especially MANETs that use today's 802.11 technology. For example, mobile phone base stations transmit at far higher power (500-1600W, but shared over all the receiving phones) than mobile nodes in MANETs (0.1-0.001W for most 802.11 cards). Even mobile phones transmit with higher power than 802.11 (1-2W for GSM). Similarly, the base station in a mobile phone network is far more sensitive than the small receiver used 802.11 cards. Consequently, second order propagation effects are significant for mobile phones, while they are less so in 802.11. Another distinction between mobile phones and MANET communication is that the mobile phone physical layer is narrow band (30kHz for D-AMPS)², while the 802.11 physical layer uses a much wider band (around 20MHz for 802.11).

The most basic model of propagation is the free space model that dictates that the received power is $P_R = P_T C / d^2$ where P_T is the transmitter power, C is a constant, and d is the distance between the transmitter and the receiver. This model is only valid when there is no ground or buildings and when the distance between the transmitter and receiver is large enough (e.g., over one meter). In all terrestrial applications, the ground is nearby and buildings are often present. Thus, the free space propagation model must be combined with other models that account for the reflective nature of ground and walls of the buildings.

While the ground and buildings do not reflect visible light very efficiently, to radio signals at the frequencies used in MANETs, the ground and buildings act as reflectors. Thus, rays emitted from the transmitter may reflect off of several buildings and the ground before reaching the receiver. In this way, several rays that are emitted from the transmitter in different directions reach the receiver. However, each of these rays takes a different path. These rays make a different number of reflections and travel different distances before reaching the receiver. As a result, a pulse that leaves the transmitter will arrive at the receiver as several pulses, each delayed and each with a different amplitude (there are also other phase differences besides that caused by delay).

The presence of these multiple rays has some important consequences for the physical layer. In narrow bandwidth communication, the quality of the communication depends on the amount of power received when the carrier frequency is transmitted. For example, suppose that the carrier frequency is f , then the received signal is $\cos(2\pi ft)$. However, if two rays take two different paths before arriving at the receiver, then the received signal is $a \cos(2\pi ft) + b \cos(2\pi f(t - L))$, where L accounts for the fact that one ray will be delayed and a and b account for the difference amplitudes. Now if $L = 1/2f$, then the received signal is $a \cos(2\pi ft) - b \cos(2\pi ft) = (a - b) \cos(2\pi ft)$. Hence, the rays tend to cancel out. On the other hand, if $L = 1/f$, then $(a + b) \cos(2\pi ft)$; the rays add. Thus, depending on the difference in the length of the paths and the frequency of the carrier, the signals may add or subtract. This situation is called multipath fading.

²CDMA is wider bandwidth.

Several stochastic models have been developed to model the effect of multipath fading. Perhaps the most popular of these are the Rayleigh and Rician models. These model the received power as a random variable and have been verified through extensive measurement. It is important to note that the value of L that causes the signals to subtract or add is very sensitive on the carrier frequency. Thus, multipath fading is usually a problem only in narrow bandwidth communication. Indeed, in order to avoid this multipath fading problem, the physical layer for MANETs uses a wide-bandwidth physical layer. In an ideal wide-band communication, equalization or some other technique is used so that, in effect, the frequencies that are not canceling out are utilized.

Multipath fading models accounts for the variation of the received signal power due to small movements of the receiver or reflective objects. Another problem is called shadowing. Like the name implies, shadowing is the decrease in received signal because a large obstacle is between the transmitter and receiver, that is, the receiver is in the shadow of an obstacle. A large number of measurements have shown that the distribution of the signal strength, when averaged over an area large enough to negate the effect of multipath fading, is distributed according to a log-normal distribution. Such models allow physical layer designers to compare the performance of one method to another. However, this model is not meant to imply that the signal strength is actually log-normal distributed. In reality, the effects of shadowing are deterministic. Indeed, the transmitter and receiver are blocked by a building or they are not. Furthermore, when the transmitter or receiver move, unless they suddenly jump to a random location, the shadowing at the next location is highly correlated with the shadowing at the last location. It would be incorrect to assume that the effect of shadowing on each packet is independent from the effect of shadowing on another packet.

Thus, for simulation of MANETs, instead of using a log-normal or any stochastic model of shadowing, a deterministic one should be used, as is done in the UDel model.

A. Ray Tracing

Ray tracing is a deterministic method that is well known for accurately predicting the received signal strength. Ray tracing tools are extensively used by wireless network planners to determine where base stations should be located [19], [20], [21]. Ray tracing models the transmitter as a source of rays departing at all angles. It determines the paths taken by these rays. In an urban area, these paths typically encounter many obstacles and hence, include many reflections. The loss along each path is also determined. Typically, the loss is due to the distance of the path along with loss for each reflection. Furthermore, second order effects such as diffraction and scattering are also included.

Because ray tracing finds the path of each ray that travels between the transmitter and receiver, it yields very accurate estimates of path loss. However, since each ray that travels between the transmitter and receiver must be found, ray tracing is extremely computationally complex. The typical approach is to trace rays that emanate from the source at a large number of finely spaced angles. For example, rays are launched at angles $0, \Delta, 2\Delta, \dots, 2\pi - \Delta$, where Δ is some small number. However, as depicted in Figure 1, such an approach can result in the rays missing an arbitrarily large area. A searching method must be used to adaptively adjust the spacing of the rays and find missed regions.

An alternative to ray tracing is beam tracing [22]. Beam tracing does not find the individual paths from transmitter to receiver, but tracks beams. With beam tracing the resolution problem of ray tracing does not exist. For this reason, the UDel models uses beam tracing.

B. Ground Reflection

As mentioned, the free space propagation model assumed that the received signal power decays like the reciprocal of the square of the distance between the source and the destination. In different environments, a better approximation is obtained by using an exponent that is different from two. Section VII illustrates a wave guide; a simple model of a wave guide has an exponent less than two. When the signal propagates through different objects, then an exponent larger than two is often appropriate. One special situation arises when there is a line-of-sight path (i.e., with no reflections) between the transmitter and receiver and a path that has a reflection off of the ground, *and the transmitter are far apart*. In this special case, these two rays combine to act like a single ray, but with an exponent equal to four. Unlike the multipath fading discussed above, the effect of the ground reflection occurs at all frequencies, hence wide-band communication will not alleviate the problem.

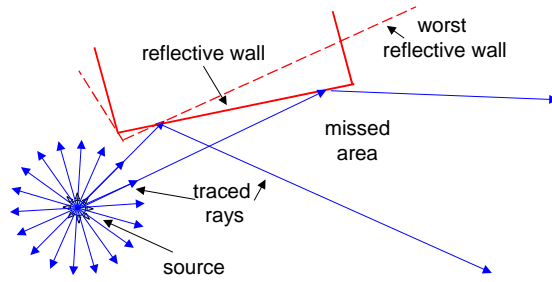


Fig. 1. Ray Tracing. The transmitter is in the lower left. Rays depart at angles spaced by 20° . The rays that reflect off of the red building miss a large area. If the building was as the dotted line shows, the error would be larger. Indeed, as the edge of the building and the source become colinear, the missed area becomes arbitrarily large.

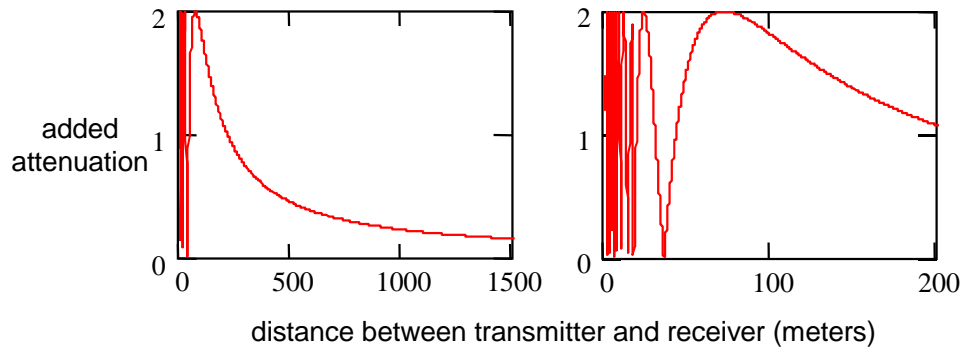


Fig. 2. The Added Attenuation due to a Ground Reflected Signal and a Line of Sight Signal. In these figures the signal is assumed to be 2.4GHz and the antenna height is 1.5 meters. The right-hand plot is a zoomed in version of the left-hand plot.

The effect of the ground reflection is well presented in many textbooks (e.g., [18]). In short, the reason that the ground reflection is more critical than other reflections is that as the distance between the transmitter and the receiver increases, the ground reflection and the line-of-sight signal arrive at the receiver nearly out of phase³, and hence cancel each other out. However, one must apply caution when employing this model. It seems that in MANETs an exponent of two is more realistic. To see this consider Figure 2. This figure shows the added attenuation due to the cancellation by the ground reflection. Thus, the actual received power is the value of the plot divided by d^2 , where d is the distance between transmitter and receiver. The figure on the left shows that for large distances, this added attenuation varies like d^2 . The result is that the total attenuation varies like d^4 . However, for smaller distance, we see that the attenuation is much less. Indeed, the signal oscillates between being amplified and attenuated. It should be noted that plot is for exactly 2.4GHz. Thus a very narrow band signal, with a frequency of exactly 2.4GHz would suffer the attenuation as shown. With proper equalization, a wider bandwidth signal would not suffer any added attenuation due to the ground reflection below 220 meters. Hence, for distances up to 500 meters, the effect of the ground reflection is less than 3dB. Since the transmission range of much of the physical layer technology is less than 500 meters (especially those that use today's 802.11 technology), it seems that an exponent of 4 is not realistic. (For mobile phones, the distances are tens of kilometers, hence the ground reflection may be more important.)

Another reason that the ground reflection must be treated with care is that this analysis is only for line of sight communication. In urban areas, with low antenna heights used in MANETs (as opposed to mobile phone base station antennas) extensive communication is not line of sight. In the case of non-line-of-sight links, the effect of the ground reflection is further complicated.

³They travel nearly the same distance, but the reflection causes a 180° phase shift.

IV. OBSTRUCTION CONE

In [12] and more recently in [10], MANET simulations included some consideration of propagation in the presence of obstacles. The idea in those papers was to model buildings not as reflective, but as perfect absorbing obstacles. In [10] this model is called *obstruction cone*. Of course, in reality, walls reflect the signal. Some examples of propagation in Section VII illustrated why the obstruction cone method is a poor approximation.

V. THE UDEL MOBILITY MODEL

The UDel mobility model has two major components, a graphical description of an urban area and mobility on this graph. These components incorporate many aspects of the models previously employed in mobility models.

A. Graphical Description of an Urban Area

Like the graph-based mobility models discussed in Section II, in the UDel mobility model mobile nodes move on a graph. However, the UDel mobility model uses graphical model of an urban area. The current version of the UDel models requires user specification of the urban area. The description is simplified in that all that is required is the locations of the buildings, the size of the buildings (including the number of floors), the orientation of the buildings, roads, and sidewalks. However, sidewalks can also be automatically generated. Preliminary work has already begun on automatic construction of the urban area as well as on a GUI. Furthermore, a library of urban areas is being developed with several models already available [1]. Visualization tools have already been developed. A screen shot is shown in Figure 4.

From a graphical perspective, the urban area is defined as vertices and adjacencies between vertices. Next we describe this graph.

1) *Buildings and Offices*: A simple and homogeneous model of buildings is employed. Specifically, a building is composed of offices and hallways. Offices are assumed to be of uniform width (a user parameter with the default set to 3 meters). Hallways run the length of the building and are oriented according to the user specified orientation. The width of the hallway is $1/3^{\text{rd}}$ of the width of the building while the offices, which lie on both sides of the hallway, have a length of $1/3^{\text{rd}}$ of the width of the building. See Figure 3.

From the graphical perspective, hallways are made up of a series of vertices; one in front of each office and one on each end of the hallway. The adjacency of the hallway vertices are defined in the obvious way. However, vertices on the ends of the hallways are also adjacent with the vertices on the floors directly above and below. Thus, these vertices act as stairways connecting the floors of the building. Each office consists of a single vertex and is adjacent to the hallway vertex directly in front of the office.

In order to make more general buildings, individual buildings can be combined into a building complex. Such groups of buildings are defined by the complex ID in the user specified configuration file. In this case, the buildings are joined as follows. If two buildings are adjacent in such a way that the end of the hallways meet, the hallways are joined by defining the vertices at the ends of the hallways to be adjacent. On the other hand, if the end of a hallway is adjacent to an office, the office vertices are redefined as hallway vertices and are defined as adjacent to the hallway vertices. And finally, if two buildings are neighbors and belong to the same building complex, and yet the hallways are not adjacent, then one office vertex from each building on each floor is redefined as a hallway vertex and adjacency is defined.

Finally, doors are defined so that they lead to sidewalks, as defined next.

2) *Sidewalks*: Walking mobile nodes (as opposed to nodes that remain on roads or remain airborne) must move along sidewalks or through buildings. Hence, in order for nodes to be able to move between arbitrary offices in arbitrary buildings, sidewalks must be defined so that buildings are properly connected. For the mobility, it is required that sidewalks exists so that a mobile node can move from one building to any other by just utilizing sidewalks. Thus, passing through a building in order to get to another building is not permitted.

This type of connectivity makes the construction of sidewalks slightly problematic. It is possible for the user to specify sidewalks. If the end of any of these sidewalks is close to a building and the end of the sidewalk is defined as a sidewalk-to-building connector, then the vertex that defines the end of the sidewalk is defined to be adjacent to the nearest vertex that is inside the building. If this nearest vertex is an office vertex, it is redefined as a hallway/door vertex.

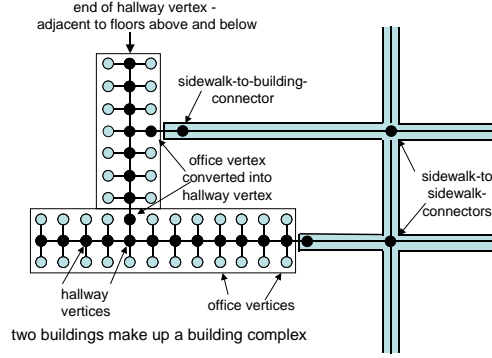


Fig. 3. A Building Complex and Sidewalk. The buildings are the large rectangular boxes. Inside the buildings are vertices that represent either offices (pale blue) or hallways (black). Outside of the buildings are sidewalks that connect the buildings together.

User defined sidewalks greatly simplify the connectivity of the buildings. However, it is tedious to define each sidewalk. Instead, if the building-sidewalk topology is not properly connected, sidewalks are automatically generated. These sidewalks originate from the center of all four sides of the buildings and grow until they reach another building or until the building-sidewalk topology is properly connected. When a sidewalk crosses another sidewalk, a vertex is defined at the intersection point and adjacencies are defined. It is possible that this process will never result in a connected topology. Furthermore, this process may result in an unrealistic number of sidewalks. In these cases, a few well-placed user defined sidewalks are required. Typically, the user defined sidewalks are trivial to define.

3) *Roads and Air Space*: While many mobile nodes move from office to office, others, such as cars, move along the roads. Roads are defined as a separate graph. Each road is assumed to begin on the edge of the modeled area and to end on an edge of the area. The road is defined by one or several straight legs. Vehicles are restricted to a single road.

Air space, occupied by helicopters, planes and UAVs, is not defined with a graph. Rather, a 3 dimensional rectangular region is defined and aircraft are restricted to this area.

B. Mobility

Multiple mobility models are utilized. Specifically, aircraft utilize a random waypoint, vehicles utilize a simple type of freeway model, pedestrians utilize either a modified graph-based random walk or a graph-based random waypoint. As discussed in Section II, the first two models have been employ previously. However, the construction is different.

1) *Pedestrian Mobility*: Two pedestrian mobility models are available, graph-based random waypoint and modified graph-based random walk. The graph-based random waypoint is similar to the graph-based random waypoint models discussed in Section II. Mobile nodes pick an office location and speed and proceed to this office at this selected speed. It is assumed that the office is selected uniformly over all offices.

A model of large urban area yields a large graph. Determining the shortest path routing between each office pair is computationally complex. Hence, a two-tier hierarchical approach is employed. The first tier consists of the buildings as destinations with sidewalks providing paths between buildings. The second tier is the buildings. Two types of shortest paths are found, paths within buildings, and paths between buildings. To relate this to the Internet, the sidewalk vertices are backbone routers, the sidewalks are backbone links, and the buildings are terminal ASs. Since buildings are treated as terminal ASs, paths between buildings do not pass through buildings (they do not carry transit traffic). For this reason, the sidewalks must provide a path between any two buildings. Shortest paths (in terms of distance, not hops) are found between buildings. Within a building, shortest path is found to door that leads to the shortest path to the destination office.

Prior to computing the itineraries of each pedestrian, all paths are found. Because the goal is to find all paths, a simple breadth first search, originating from a single source, yields optimal paths to destinations. Once all paths are found, graphical random waypoint mobility is easily implemented in a computationally efficient manner. Mobility for 2000 mobile nodes for 2000 seconds for the city shown in Figure 4 took less than five minutes on a Pentium 4 running at 2.4GHz with 512MB memory. Note that not all of the city can be seen in Figure 4.

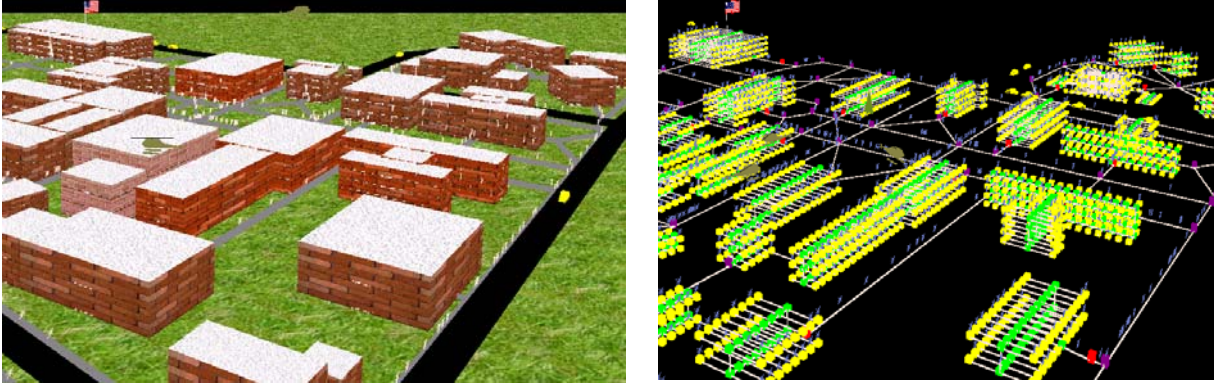


Fig. 4. Graphical Description of an Urban Environment. The yellow blobs are cars (more easily seen in the left-hand plot), the green blobs are helicopters, and the pedestrian mobile nodes are depicted as white asterisks on the left and blue on the right. Careful examination of the right-hand plot shows that many of the office are occupied while many nodes also move along sidewalks.

Like other mobility models, the graph-based random waypoint restricts the node to pause at its destination (office) for a random amount of time. This time can be either exponentially, Pareto, or uniformly distributed.

The modified graph-based random walk is similar to other random walk models described in Section II. Specifically, when a pedestrian reaches a vertex, be it a sidewalk vertex or hallways vertex, a random selection is made as to which neighboring vertex to visit next. There are two significant differences between graph-based random walk of Section II and the one presented here. First, here pedestrians do not "pause" at every node of the graph. Rather, the pauses are restricted to the office nodes. Second, the next destination is not selected uniformly or in a memoryless way. That is, when a node reaches a hallway vertex outside an office, it does not select proceeding down the hallway, entering the office or backtracking in the hallway with equal probability. It is not hard to see that if this was the case, vertices would very rarely leave buildings with a large number of offices, and when they did, it would only be after visiting a huge number of offices. As a result, uniform random walk yields an unrealistic mobility. Another unrealistic characteristic of the pure random walk is that nodes have a tendency to backtrack and roam through buildings, as oppose to exit buildings and have a tendency to enter buildings (without backtracking).

In order to generate more realistic mobility, the following ad hoc scheme was devised and found to work well. The goal is to avoid entering into offices, avoid backtracking and tend to exit the building. These goals are met by selecting from the adjacent vertices with nonuniform probabilities that depend on the path taken by the mobile. Specifically, for each neighboring vertex i we find weight w_i and then select node i with probability $w_i / \sum_{j=1}^N w_j$, where N is the number of neighbors. The weight w_i is found by first determining a variable u_i as follows. If the neighboring vertex is an office vertex and the pedestrian has been in an office in the last ten steps, then we set $u_i = 0.00002$. If the vertex is a sidewalk-to-building-connector, then $u_i = 2$. Otherwise, $u_i = 1$. Now, if the pedestrian has visited the neighboring vertex within the past 15 steps, this vertex is given a weight $w_i = u_i \times 1.84^{\text{NumSteps}}$, where NumSteps is the number of steps since this vertex was visited. If this vertex has not been visited in the past 15 steps, the weight is set to $w_i = u_i$.

The UDel mobility model allows pedestrians to follow a modified random walk or random waypoint. It is possible to have different types of mobility in the same simulation.

2) *Other Mobility Patterns:* The UDel mobility model includes aircraft and vehicles. Aircraft follow a simple random waypoint and are restricted to remain in a three dimensional rectangle. It is assumed that the aircraft would be some type of UAV to provide radio support. Since such UAVs might follow a periodic path, it is allowed that the random waypoint trajectory repeat itself after a user specified number of steps.

Vehicles are assumed to follow roads. The vehicles select a road at random and a speed at random. Once the vehicle reaches the end of the road, the vehicle can either pause (but no longer be included in the ad hoc network) for an exponentially distributed amount of time, or immediately select a new road. The random version allows for the number of vehicles that are passing through the area to be variable.

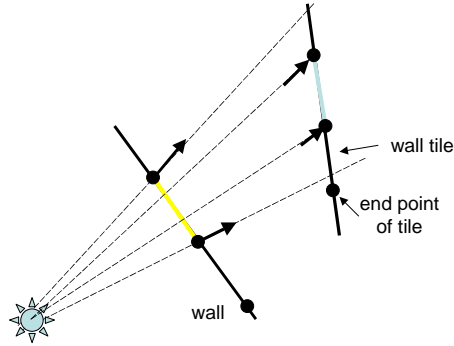


Fig. 5. Beam Tracing. Suppose that the (yellow) tile on the lower left has been determined to have been hit by the beam. In particular, this beam hits the end points such that the reflected rays are as shown. From these rays, the virtual source, shown in the lower right is found. The angle at which the beam hits the end points of the (blue) tile in the upper right is found as shown. These rays as translated into reflected rays according to Snell's Law and the process continues.

VI. THE UDEL PROPAGATION MODEL

As discussed in Section III, stochastic propagation models are not appropriate for simulation of MANETs. Instead, we develop a deterministic site specific model. The outdoor model uses two-dimensional beam tracing, while the indoor model uses an *attenuation factor (AF) model*. The complete propagation model uses a mixture of beam tracing and the AF model.

A. Beam tracing

As discussed in Section III, beam tracing is similar to ray tracing. The source broadcasts the signal in all directions. We can model this transmission as the broadcast of a group of beams with the combination of the beams spanning all directions. When a beam intersects an object, it is reflected. However, if only part of the beam intersects the object, the beam is split into two, with one beam continuing and the other beam reflecting. Finally, if the receiver is found to be included within the span of a beam, the contribution of this beam toward the total received power can be determined.

The UDel model provides propagation loss between every source-destination pair. However, to ease the computational complexity, the space was divided into a grid and the path loss between the center points of each square of the grid was found.

The computation is divided into two parts, preprocessing and beam tracing. In order to speed up the beam tracing, each wall was divided into tiles. We call these tiles *wall tiles*. Then, during preprocessing, the *ray neighbors* for each tile were found. Tiles are ray neighbors if it is possible that a ray coming from one tile could hit the other tile. For each ray neighbor of a tile, it is found at what angles a ray departs from the tile in order to hit its neighbor. To allow for rapid searching, the list of ray neighbors is ordered by departing angle of the ray.

As mentioned, space is divided into a grid. We call each square of the grid a *floortile*. We also determine which of the floor tiles can be reached from a wall tile. The list of these floor tile neighbors is also precomputed for each wall tile.

Once the ray neighbors are found, beam tracing can be performed efficiently. The first step is to identify which wall tiles are intercepted by the rays emanating from the source. Then the angles that the rays hit the edges of the tiles are determined. These angles and the list of ray neighbors are used to determine which tiles the reflected beam will next strike. Once the next tiles are found, the angles that the rays hit the edges of these tiles are found and the process continues. Figure 5 shows how this computation is performed.

B. Indoor Propagation

While beam tracing can be used to determine indoor propagation, it tends to be computationally complex. Instead, an *attenuation factor model* was employed [18]. While it is possible to use beam tracing for indoors, this would be

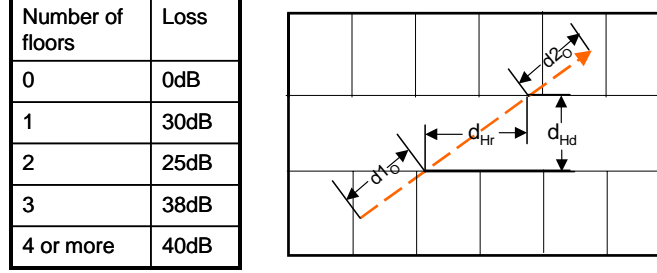


Fig. 6. Right. Added Loss from Passing Through Floors. Left. Indoor Propagation. The above path passes through five interior walls.

computationally complex and since indoor propagation is dependent on small scale objects such as the placement of desks and file cabinets, indoor beam tracing might not be significantly more realistic than the AF model. In [18], such models are reported to provide loss within 4dB when compared to the actual loss in the building that is modeled. This model breaks the path loss into three factors, attenuation from through an office or hallway, propagation through a wall, and propagation through a floor.

The AF model provides the path loss along the direct, straight line path between transmitter and receiver. Let n be the number of walls that this straight line path passes, m be the number of floors that this path passes, d_O the distance through offices that this path passes, and let d_{Hr} be the distance through the hallway and parallel to the hallway while d_{Hd} is the distance through the hallway but perpendicular to the hallway. Then, the path loss in dBm (dB meters) along this path is

$$PL = \alpha_O 10 \log(d_O) + \alpha_R 10 \log(d_{Hr}) + \alpha_D 10 \log(d_{Hd}) + WL \times n + FL(m),$$

where α_O is the attenuation exponent through an office and is taken to be between 1.8 and 3 (See Table 4.6 in [18]). α_R is the attenuation exponent along a hallway. Since hallways act as wave guides, this path loss exponent is often below two, with common values between 1.6 and 1.8 [23]. α_D is the attenuation exponent perpendicular to a hallway and is taken to be in the same range as the exponent in an office. Left-hand plot in Figure 6 shows how these distances are related. WL is the loss through a wall. Table 4.3 in [18] gives this value to be between about 2dB for a sheetrock wall to 8 - 20 dB for a concrete or concrete block wall. FL is the attenuation through a floor. Tables 4.3, 4.4 and 4.4 in [18] show that this value is between 10-30dB for one floor ($m = 1$). However, as the number of floors increases, added loss per floor decreases. While the values can be changed, the default relationship between loss and floors is given by the table shown in Figure 6.

C. The UDel Propagation Model

Beam tracing and the AF model are the two main components of the UDel propagation model. Outdoors, beam tracing is used to determine the paths of rays. Each reflection is assumed to result in a loss of L_C and result in a penetration into the building with a loss of $L_{\bar{C}}$. By default $L_{\bar{C}} = 10 \log(1 - 10^{-L_C/10})$, hence, the wall is assumed to not absorb any power. $L_{\bar{C}}$ is taken to be around 13-16dB as discussed in Section 4.12 of [18]. The loss along a path that is always outdoors is $L_C \times \text{NumberOfReflections} + \alpha_F 10 \log(d)$, where d is the length of the path. By default, the attenuation exponent α_F is 2, as discussed in Section III-B.

As mentioned, when a beam strikes a wall, some of the signal penetrates into the building after suffering around 13dB of loss. The propagation through the building is modeled using beam tracing and the AF model. It is assumed that only the edge walls of the building reflect the signal. From the point of entry into the building, to the point where the signal strikes another edge wall of the building, the signal suffers a loss given by AF model. Similarly, if a beam reaches a destination within the building, the loss from the point of entry to the receiver follows the AF model. It should be noted that in many cases, due to the loss of power as a signal passes through a building, the reflections within a building have a minor effect of the received signal strength.

The current version of the UDel propagation model does not include 3-D effects. Thus all beam tracing is restricted to a plane. In order to accommodate buildings with multiple floors, the following approximation is used. If a transmitter and receiver are in the same building, then the AF model provides the loss along the direct path

from transmitter to receiver. However, if a signal exits the building, we always assume that this signal propagates at all heights. Thus, if this signal strikes another building, it is assumed that signal penetrates into all floors with equal strength. This implies that a signal may start in the fourth floor of a building, exit the building, reflect off of a nearby building and reenter the building of the transmitter and reach a receiver on the first floor. Such a transmission would be affected by the attenuation due to the number of floors between the transmitter. However, the signal does have to propagate through the building twice (once to the edge wall and once from the edge wall), pass through the wall twice, and propagate to and back from a nearby building. Nonetheless, such paths may provide less loss than the direct paths that must pass through multiple floors.

VII. EXAMPLES

In this section we present some examples that illustrate the features of the UDel propagation model. Figure 7 shows the path loss with the transmitter in two different places. It can be seen that because of reflections, reasonable high signal strength is found in many areas that one might not have initially suspected. Note that in the left-hand plot, there is a large region where a strong signal will be received (the orange). However, the right-hand shows a much smaller region with good propagation. The common assumption that locality implies connectivity seem not to hold. Similarly, it seems that speed would likely not be a good indicator of the residual lifetime of a link. These issues must be investigated and quantified.

The left-hand plot in Figure 8 shows the effect of a waveguide formed by an alleyway between two buildings. Note that transmitter is on the far right of the alleyway. However, the signal strength on the far left of the alleyway is as high as it is at points near to the transmitter. On the other hand, the signal strength to the right of the transmitter decays quite rapidly. The reason for this behavior is that because of the reflections, the signal is focused down the alleyway. The walls are mostly reflective. Thus there is no place else for the energy to go but down the alleyway. Also notice the effect of the subtle difference in the building lengths.

The right-hand plot in Figure 8 shows how the signal propagates through buildings. These buildings are oriented so that the hallways run horizontally. Notice that in the building on the left, the signal propagates down the hallway. As discussed in [23], the waveguide effect causes the attenuation exponent down a hallway to be less than two. In this case, we see that the propagation down the hallway is efficient enough that there is some signal strength on the backside of the building. The propagation through the other buildings is quite complex. In the case of the building in the upper right, we see that directly in front of the transmitter, the signal propagates further into the buildings than in other places. This is due to the propagation through an office into the hallway. Such propagation only has to pass through two walls. However, when the signal enters on an angle, the signal must propagate through walls that divide offices. Hence, in this direction, the signal does not propagate very far. Finally, in the lower right, we see again a small effect of the good propagation properties of hallways.

Figure 9 shows the propagation from a transmitter inside a building. We see that very little signal is able to pass through the building to the outdoors. Furthermore, the propagation to other floors, especially many floors away, is limited. Similar to right-hand plot in Figure 8, these figures also show effect of hallways and offices. Specifically, we see that the signal is able to propagate down the hallway more efficiently than through offices. Furthermore, the signal can propagate to the office directly across the hallway much better than to other offices on as well.

The computational complexity is a major concern for ray tracing and related techniques. However, while we have identified several optimizations that would improve the run time of the path loss computation, the computation is fairly reasonable in its current form. The precomputation is single processor code, while the path loss can be performed on a single processor or, using MPI, on multiple machines. Table 1 shows the computation time for different environments. These computations used machines with 2.4GHz Pentium 4 with 512MB memory. The path loss for the first two environments was performed on three machines and the third path loss calculation was carried out with four machines. While not a quick calculation, the calculation of path loss is feasible. Once the path loss is determined, it can be used with any mobility. We are not only developing an archive of graph-based environments, but developing an archive of path loss calculations. These will be available for downloading.

VIII. MANET PERFORMANCE UNDER THE UDEL MODELS

The main focus of this paper is to introduce the UDel models. However, a brief discussion of the impact that these models have on performance can be briefly discussed. To this end, the QualNet simulator was used to perform

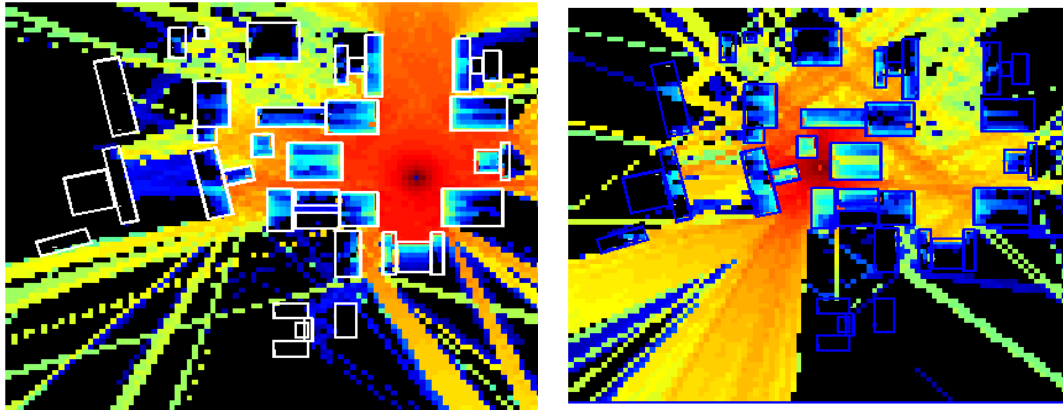


Fig. 7. Path Loss in an Urban/Suburban Environment. The dark red indicates low path loss (high signal strength). The yellow indicates higher path loss and black indicates path loss over 100dB. The buildings are shown with a white outline on the left and a blue outline on the right.

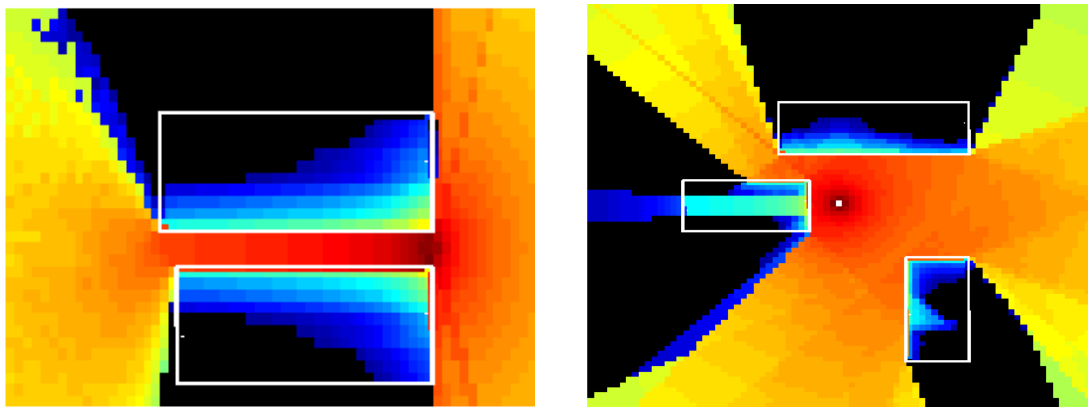


Fig. 8. Right. Propagation Down an Alleyway. The buildings are indicated in white. The transmitter is on the right side of the alleyway. Left. Propagation into Buildings. The transmitter is indicated by the white dot.

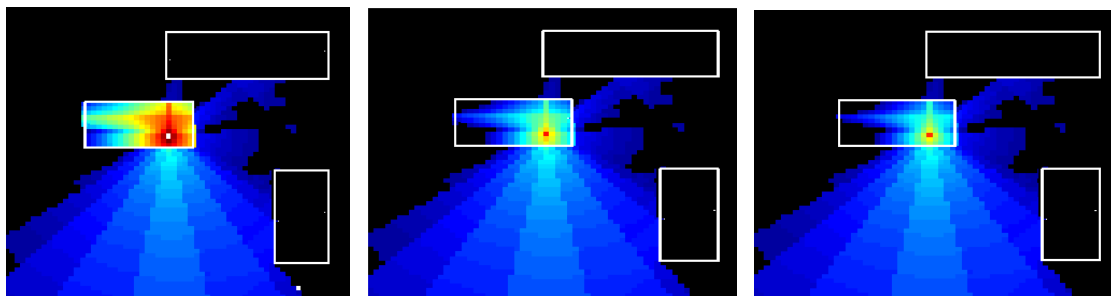


Fig. 9. Path Loss from Inside a Building. The building is indicated with the white outline. The transmitter is on the first floor of the building. The figure on the left shows the loss on the first floor of the building as well as in the area around the building. The middle and right-most plots shows the path loss on the second floors and third floors as well as in the area around the building.

Environment	Precomputation Time	Path Loss Time
4 buildings 524 wall tiles 16 walls 5640 floor tiles 2360 interior floor tiles	158 seconds	24900 seconds
19 buildings 1314 wall tiles 76 walls 2347 floor tiles 1879 interior floor tiles	170 seconds	7367 seconds
18 buildings 1625 wall tiles 72 walls 3125 floor tiles 1309 interior floor tiles	296 seconds	12823 seconds

Fig. 10. Table 1

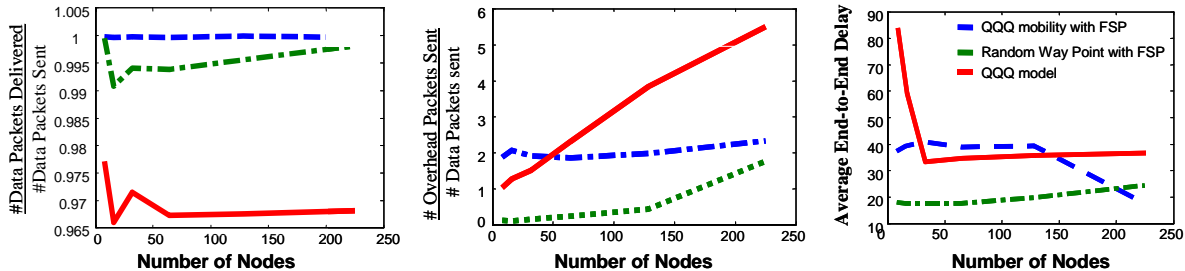


Fig. 11. Simulation Results.

simulations under three environments, free space propagation with random waypoint, UDel graph-based mobility with free space propagation, and the full UDel models. In these experiments, the number of nodes varied by powers of 2 from 8 to 256. There were seven sources each sending CBR data at a rate of four packets/sec. The packet size was 512B. The simulation area was 1200m×1200m. The mobile nodes (pedestrians) velocity ranged from 0.2m/s to 0.08m/s. There was no pause time. AODV was used for all simulations. In each setting, ten simulations were performed.

Figure 11 shows the results of these simulations. We see a dramatic difference in the behavior of AODV under the different simulation settings. In particular, as compared to random waypoint and free space models, the UDel model results in a smaller packet delivery ratio, a increase in routing overhead by a factor of six, and an increase in end-to-end delay by 50-75%. Note that these differences are most significant when the full UDel model is used. Hence, the difference is due to both the mobility and the path loss model.

Figure 12 shows another view of the impact of the UDel modeling environment. Here we suppose that links exists only if the path loss is less than 70dB. In QualNet, the default threshold is 105dB. However, in reality, a higher bit-rate links require less path loss. Given the threshold of 70dB, we computed the number of connected components as a function of time. Figure 12 shows this time series as well as the autocorrelation. Both plots show that when compared to the UDel mobility model with free space propagation, the full UDel model induces more abrupt changes in the connectivity of the network. It is likely that this rapid variation is the reason that AODV performed significantly poorer under the UDel models as compared to the random waypoint free space model.

IX. CONCLUSIONS AND FUTURE WORK

The UDel models are a new direction in MANET simulators. Not only do the UDel models include a new mobility model, but these models allow path loss to be easily incorporated into simulations. Ongoing research is focused on understanding the full impact of path loss.

While the UDel models do provide a model for path loss, there is much more work to be done to improve the fidelity of these models. This work is ongoing and, in the future, promises to account for ground reflections,

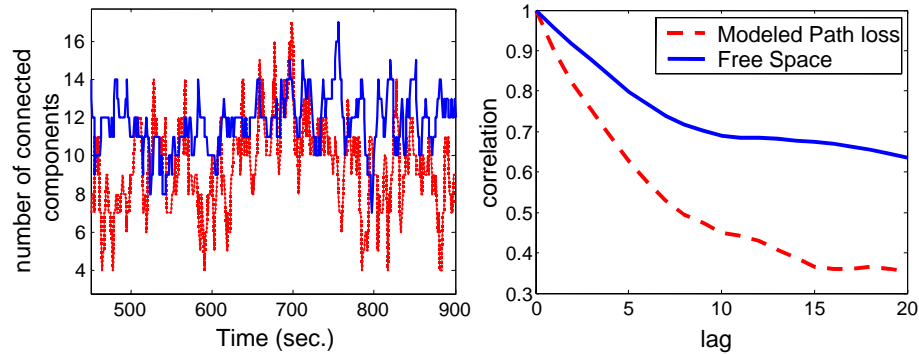


Fig. 12. Connectivity. The right-hand plot is the autocorrelation of the time series of number of connected components shown in the left-hand plot. Note that the path loss model causes the correlation to decrease, that is, the connectivity is less predictable.

diffraction, random terrain (hills etc.), scatter due to small objects such as people, trees and cars, utilize full 3-D beam tracing, and study of the building interior model. While much work remains, the models are mature enough to be utilized by the MANET research community. Another area to be investigated is the validation of the model. However, the building blocks of this model are from the literature and have been extensively verified. Hence, no significant changes in the model are expected to result from measurements. Nonetheless, validation will be performed.

The UDel plot can provide a detailed view of the link. In particular, it can provide a picture of each path complete with the angles of impact on reflective surfaces, launch angle from the transmitter and arrival angle at the receiver, and of course, distance of the path. Thus, these tools are useful for directional antennas and ultrawide-band propagation models.

Finally, the mobility model will be extended to include group mobility and scenario mobility.

REFERENCES

- [1] Web page withheld for confidentiality, ,” Tech. Rep.
- [2] S. R. Das, A. Mukherjee, B. Bandyopadhyay, and D. Saha K. Paul, “Improving quality-of-service in ad hoc wireless networks with adaptive multi-path routing,” in *IEEE Globecom 2000*, 2000.
- [3] R. Dube, C. D. Rais, K.-Y. Wang, and S. K. Tripathi, “Signal stability based adaptive routing (SSA) for ad-hoc mobile networks,” *IEEE Personal Communication*, 1997.
- [4] W. Su, S. Lee, and M. Gerla, “Mobility prediction and routing in ad hoc wireless networks,” *International Journal of Network Management*, 2000.
- [5] He Dajing, Jiang Shengming, and Rao Jianqiang, “A link availability prediction model for wireless ad hoc networks,” in *Proceedings of the International Workshop on Wireless Networks and Mobile Computing*, 2000.
- [6] T. Camp, J. Boleng, and V. Davies, “A survey of mobility models for ad hoc network research,” *Wireless Communications and Mobile Computing (WCMC): Special issue on Mobile Ad Hoc Networking: Research, Trends and Applications*, vol. 2, no. 5, pp. 483–502, 2002.
- [7] Josh Broch, David A. Maltz, David B. Johnson, Yih-Chun Hu, and Jorjeta Jetcheva, “A performance comparison of multi-hop wireless ad hoc network routing protocols,” in *Mobile Computing and Networking*, 1998, pp. 85–97.
- [8] V. Tolety, “Load reduction in ad hoc networks using mobile servers,” Master’s thesis, Colorado School of Mines, 1999., 1999.
- [9] F. Bai, N. Sadagopan, and A. Helmy, “Important: a framework to systematically analyze the impact of mobility on performance of routing protocols for adhoc networks,” 2003.
- [10] Amit Jardosh, Elizabeth M. Belding-Royer, Kevin C. Almeroth, and Subhash Suri, “Towards realistic mobility models for mobile ad hoc networks,” in *Proceedings of the 9th Annual International Conference on Mobile Computing and Networking (MobiCom)*, 2003.
- [11] Xiaoyan Hong, Mario Gerla, Guangyu Pei, and Ching-Chuan Chiang, “A group mobility model for ad hoc wireless networks,” in *Proceedings of the 2nd ACM International Workshop on Modeling, Analysis and Simulation of Wireless and Mobile Systems*, 1999, vol. 2.
- [12] Per Johansson, Tony Larsson, Nicklas Hedman, Bartosz Mielczarek, and Mikael Degermark, “Scenario-based performance analysis of routing protocols for mobile ad-hoc networks,” in *Proceedings of the 5th Annual ACM/IEEE International Conference on Mobile Computing and Networking (MobiCom)*, 1999.
- [13] N. Sadagopan, B. Krishnamachari F. Bai, and A. Helmy, “Paths: Analysis of path duration statistics and their impact on reactive manet routing protocols,” in *MobiHoc*, 2003.
- [14] C. Bettstetter, “Smooth is better than sharp: A random mobility model for simulation of wireless networks,” in *Proceedings of the 4th ACM International Workshop on Modeling, Analysis and Simulation of Wireless and Mobile Systems*, 2001.
- [15] D. Blough, G. Resta, and P. Santi, “A statistical analysis of the long-run node spatial distribution in mobile ad hoc networks,” *ACM/Kluwer Wireless Networks*, 2002.
- [16] Mineo Takai, Jay Martin, and Rajive Bagrodia, “Effects of wireless physical layer modeling in mobile ad hoc networks,” in *Proceedings of the 2nd ACM International Symposium on Mobile Ad Hoc Networking and Computing (MobiHOC)*, 2001.

- [17] J. D. Parsons, *The Mobile Radio Propagation Channel*, Wiley, New York, 2000.
- [18] T. Rappaport, *Wireless Communications - Principles and Practice*, Prentice Hall, 2002.
- [19] A.R. Nix, G.E. Athanasiadou, and J.P. McGeehan, "Predicted HIPERLAN coverage and outage performance at 5.2 and 17 GHz using indoor 3-d RayTracing techniques," *Wireless Personal Commuications*, vol. 3, pp. 365–388, 1996.
- [20] D. J. Cichon, T. Kürner, and W. Wiesbeck, "3D ray optical propagation modelling in rural and urban environments and derived radio channel characterization," in *Proc. Of the 3rd ESA European Workshop on Electromagnetic Compatibility and Computational Electromagnetics*, 1993.
- [21] K. Heiska and A. Kangas, "Microcell propagation model for network planning," *Personal, Indoor and Mobile Radio Communications*, vol. 1, pp. 148–152, 1996.
- [22] Paul S. Heckbert and Pat Hanrahan, "Beam tracing polygonal objects," in *Computer Graphics (SIGGRAPH '84 Proceedings)*, Hank Christiansen, Ed., 1984, vol. 18, pp. 119–127.
- [23] Jean-Paul M. G. Linmartz, *Wireless Communication, The Interactive Multimedia CD-ROM*, Baltzer Science Publishers, P.O.Box 37208, 1030 AE Amsterdam, 1996.